RESEARCH

Check for updates

Epigenetic priming improves salvage chemotherapy in diffuse large B-cell lymphoma via endogenous retrovirus-induced cGAS-STING activation

Jun Liu[1,2,3,4], Suji Min[2], Dongchan Kim[2,4], Jihyun Park[2,4], Eunchae Park[2,4], Youngil Koh[2,4,5,6], Dong-Yeop Shin[2,4,5,6], Tae Kon Kim[7], Ja Min Byun[2,4,5,6], Sung-Soo Yoon[2,4,5,6] and Junshik Hong[2,4,5,6]*

Abstract

Background Although most patients with diffuse large B-cell lymphoma (DLBCL) achieve complete remission after first-line rituximab-containing immunochemotherapy, up to 40% of patients relapse and require salvage therapy. Among those patients, a substantial proportion remain refractory to salvage therapy due to insufficient efficacy or intolerance of toxicities. A hypomethylating agent, 5-azacytidine, showed a chemosensitizing effect when primed before chemotherapy in lymphoma cell lines and newly diagnosed DLBCL patients. However, its potential to improve outcomes of salvage chemotherapy in DLBCL has not been investigated.

Results In this study, we demonstrated the mechanism of 5-azacytidine priming as a chemosensitizer in a platinum-based salvage regimen. This chemosensitizing effect was associated with endogenous retrovirus (ERV)-induced viral mimicry responses via the cGAS-STING axis. We found deficiency of cGAS impaired the chemosensitizing effect of 5-azacytidine. Furthermore, combining vitamin C and 5-azacytidine to synergistically activate STING could be a potential remedy for insufficient priming induced by 5-azacytidine alone.

Conclusions Taken together, the chemosensitizing effect of 5-azacytidine could be exploited to overcome the limitations of the current platinum-containing salvage chemotherapy in DLBCL and the status of cGAS-STING has the potential to predict the efficacy of 5-azacytidine priming.

Keywords DLBCL, 5-Azacytidine, ERVs, STING, Cisplatin

*Correspondence:
Junshik Hong
hongjblood@snu.ac.kr
[1] College of Medicine, Zhejiang University, Hangzhou, China
[2] Center for Medical Innovation, Seoul National University Hospital, Seoul National University College of Medicine, Seoul, Republic of Korea
[3] Liangzhu Laboratory, Zhejiang University Medical Center, Hangzhou, China
[4] Cancer Research Institute, Seoul National University College of Medicine, Seoul, Republic of Korea
[5] Department of Internal Medicine, Seoul National University Hospital, Seoul National University College of Medicine, 101 Daehak-ro, Jongno-gu, Seoul 03080, Republic of Korea
[6] Biomedical Research Institute, Seoul National University College of Medicine, Seoul, Republic of Korea
[7] Division of Hematology/Oncology, Department of Internal Medicine, Vanderbilt University Medical Center, Nashville, TN, USA

Background

Diffuse large B-cell lymphoma (DLBCL) is the most common histologic subtype of non-Hodgkin lymphoma (NHL) [1]. Approximately 60–70% of patients with DLBCL achieve complete remission with first-line regimens, such as rituximab, cyclophosphamide, doxorubicin, vincristine, and prednisone (R-CHOP) [2]. However, up to 40% of patients have disease relapse or are refractory to their initial therapy [3]. For those patients, salvage chemotherapy is required, but the majority of patients succumb to their disease or require high-dose chemotherapy with autologous stem cell transplantation (ASCT) because of the limited efficacy of salvage treatment [4]. Newer treatment strategies including targeting B-cell surface antigen CD79 and chimeric antigen T-cell (CAR-T) therapy improved outcomes of those relapsed or refractory DLBCL patients [5, 6]. Polatuzumab vedotin, a monoclonal antibody-drug conjugate targeting CD79, received Food and Drug Agency approval in combination with bendamustine and rituximab (pola-BR), based on an open label clinical trial which showed superior response rate of pola-BR compared to BR [7]. However, the benefit of pola-BR was demonstrated only in transplant-ineligible patients. In addition, extra-ordinary costs make the wider use of CAR-T difficult. Thus, salvage chemotherapy followed by autologous hematopoietic cell support is still the mainstay of the second chance for cure in relapsed or refractory DLBCL patients. However, salvage chemotherapy and high-dose chemotherapy inevitably cause substantial toxicities, especially in elderly or frail patients who cannot tolerate these regimens [8]. Therefore, potentiating the effect of chemotherapy without significant toxicities is required.

Epigenetic modulators, such as hypomethylating agents, have been used to treat patients with myelodysplastic syndrome (MDS) or acute myeloid leukemia (AML). The mechanism of action underlying the clinical efficacy of 5-azacytidine remains to be elucidated [9]. To date, most of the focus on the mechanisms of action of DNA methyltransferases inhibitor (DNMTi) has been on the reversal of acquired aberrant DNA methylation of tumor suppressor; however, interest has now switched to the role of activation of endogenously methylated sequences such as the cancer–testis antigens (CTAs) and ERVs [10]. Previous data have suggested 5-azacytidine-mediated irreversible inactivation of DNA methyltransferases (DNMTs) followed by restoration of aberrantly methylated tumor suppressor genes (TSGs) as a major mechanism [11]. However, global DNA demethylation by 5-azacytidine is not correlated with clinical objective response [12]. More recently, it has been reported that low-dose 5-azacytidine and its deoxy derivative, decitabine (also known as 5-aza-2'-deoxycytidine), mediate double-stranded RNA (dsRNA) formation, which activates the pattern recognition receptor MDA5 [13]. Specifically, low-dose 5-azacytidine treatment reactivates previous epigenetic silencing of ERV element expression in the human genome. The activated ERV element forms dsRNA, which is recognized by dsRNA sensors as viral genetic material. This low-dose 5-azacytidine treatment tricks cancer cells into behaving as virus-infected cells to generate a so-called viral mimicry state [14]. Viral mimicry induces an interferon (IFN) response, which is responsible for sensitization to subsequent chemotherapy or immune checkpoint therapy [15].

Epigenetic modifications, such as DNA methyltransferase inhibition and histone deacetylase inhibition, cause sensitization to the cytotoxic effects of chemotherapeutic drugs in solid tumors [16]. The hypomethylating agents 5-azacytidine and decitabine restore the efficacy of platinum derivatives in several types of cancer cell lines in vitro [17], and this chemosensitization has been evaluated in clinical trials [18]. Hypomethylating agent-induced chemosensitization is exerted via the reprogramming of cancer cells without altering the DNA sequence and causing DNA demethylation with minimal DNA damage. This non-cytotoxic mechanism is valuable because hypomethylating agents improve sensitivity to salvage chemotherapy but do not increase toxicity in DLBCL cells [19, 20]. These advantages could lead to the use of hypomethylating agents to overcome refractoriness to platinum derivative-containing salvage chemotherapy for DLBCL without additional treatment toxicity, thereby increasing the overall survival of relapsed/refractory DLBCL patients and allowing more patients to proceed to ASCT. In this study, we elucidated the effect and mechanism of 5-azacytidine as a potential chemosensitizer in cisplatin-resistant DLBCL cells.

Results

5-Azacytidine pretreatment resensitizes cisplatin-resistant DLBCL cell lines to cisplatin to varying degrees

A platinum-based anti-neoplastic agent is an essential component of salvage regimens for aggressive lymphomas, for example, rituximab, gemcitabine, dexamethasone, and cisplatin (R-GDP) for relapsed/refractory DLBCL and Hodgkin lymphoma [21]. As a single agent in humans, cisplatin is administered at a dose of up to 80 mg/m^2, which can achieve an approximately 14.4 μM plasma peak concentration with a plasma half-life of 0.44 h [22]. The clinically achievable concentration of cisplatin was determined to be 7 μM by pharmacokinetic simulation (Fig. 1A). Thus, the sensitivity of six DLBCL cell lines to cisplatin was defined with a cutoff of 7 μM in our study. Among the six DLBCL cell lines, three (OCI-LY3, Toledo, and OCI-LY19) were sensitive to cisplatin,
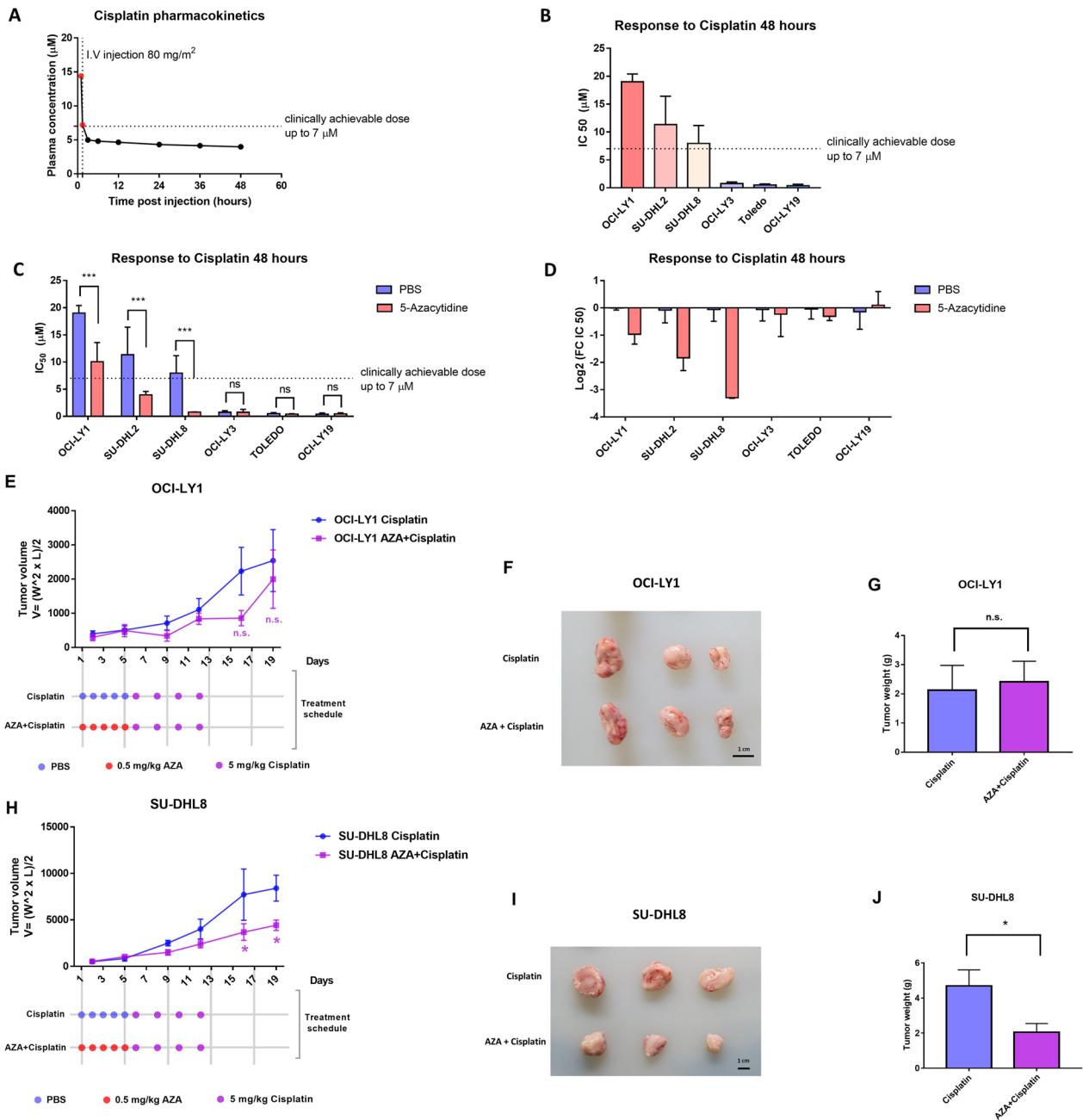
Fig. 1 5-Azacytidine pretreatment resensitizes cisplatin-resistant DLBCL cell lines to cisplatin to varying degrees. **A** Plasma levels of cisplatin in human patients following intravenous injection of an 80 mg/m² dose. Red points represent the determined value for the patient at that time point reported by a widely cited paper. Black points represent the mPBPK model-predicted value using typical physiological and biochemical parameters. The dashed line indicates the top clinically achievable dose. **B** The IC50 value was calculated using a cell viability assay. The dashed line indicates the top clinically achievable dose. **C** Bar chat of IC50 values for cisplatin in six DLBCL cell lines; *$p < 0.05$, **$p < 0.01$ and ***$p < 0.001$ (two-way ANOVA). **D** Bar chat of log2-transformed IC50 fold change values. **E**–**J**. Subcutaneous tumor growth, xenograft tumor images and tumor weights of xenografts from OCI-LY1 and SU-DHL2 tumor-bearing athymic nude mice. **E** and **H** *$p < 0.05$, **$p < 0.01$ and ***$p < 0.001$ (two-way ANOVA). **G** and **I** *$p < 0.05$, **$p < 0.01$ and ***$p < 0.001$ (*t* test). AZA: 5-azacytidine

and the other three (OCI-LY1, SU-DHL2, and SU-DHL8) were resistant (Fig. 1B), according to cisplatin half-maximal inhibitory concentration (IC50) values of each lines.

To determine whether 5-azacytidine could overcome resistance to cisplatin in DLBCL cell lines, the six DLBCL cell lines were incubated for three consecutive days with

low-dose (0.3 µM) 5-azacytidine prior to cisplatin treatment in vitro (Additional file 1: Fig. S1A). A cell viability assay showed that 5-azacytidine enhanced cisplatin sensitivity in all three resistant DLBCL cell lines (Fig. 1C, Additional file 1: Fig. S2A–F). Although all three resistant DLBCL cell lines showed a significant increase in sensitivity, only the SU-DHL2 and SU-DHL8 cell lines regained cisplatin chemosensitivity and exhibited IC50 values below the clinically achievable concentration (Fig. 1C). By comparing the cisplatin IC50 values measured with or without 5-azacytidine pretreatment, we found that the resistant DLBCL cell lines received different degrees of benefits from this epigenetic priming: SU-DHL8 cells gained the most benefit, followed by SU-DHL2 cells, and OCI-LY1 cells gained the least benefit (Fig. 1D).

We then performed an in vivo study to evaluate the efficacy of 5-azacytidine in sensitizing the effect of cisplatin using xenograft models (Additional file 1: Fig. S1B). In the OCI-LY1 xenograft model, 5-azacytidine pretreatment augmented the effect of cisplatin on day 16, although it was not statistically significant ($p = 0.1898$, two-way-ANOVA) (Fig. 1E). However, this inhibitory trend was not sustained beyond day 19 (Fig. 1E–G). In contrast, 5-azacytidine epigenetic priming significantly increased the cytotoxic effect of cisplatin on day 16 ($p = 0.046$, two-way-ANOVA), and moreover, this combination effect was durable in the SU-DHL8 xenograft model on day 19

($p = 0.049$, two-way-ANOVA) (Fig. 1H–J). The responses of the in vivo studies in Fig. 1E, F, G, H, I, and J correlate with the level of cisplatin resistance in Fig. 1B, C, and D. Adding 5-azacytidine to OCI-LY1 cells did not have a significant effect in vivo but it did to SU-DHL8, which were sufficiently primed by 5-azacytidine in Fig. 1B, C, and D. Taken together, these data suggested that 5-azacytidine epigenetic priming augmented the cytotoxic response to cisplatin in cisplatin-resistant DLBCL cell lines to varying degrees, to be specific, most significant on SU-DHL8 and almost negligible on OCI-LY1. The mechanism underlying this phenomenon has been investigated in the following experiments.

Low-dose 5-azacytidine induces DNA demethylation without DNA damage

To determine whether 5-azacytidine-induced chemosensitization is dependent on DNA damage, the DNA damage marker phospho-H2AX was evaluated each day after 5-azacytidine treatment. Three consecutive days of low-dose 5-azacytidine treatment had negligible impacts on phospho-H2AX (Fig. 2A). Three consecutive days of low-dose 5-azacytidine treatment decreased the global DNA methylation level, detected using 5-methylcytosine (5mC) DNA dot blotting, in all six DLBCL cell lines (Fig. 2B). In addition, low-dose 5-azacytidine treatment decreased the DNMT1 protein levels in all six DLBCL cell lines (Fig. 2C). These data indicated that
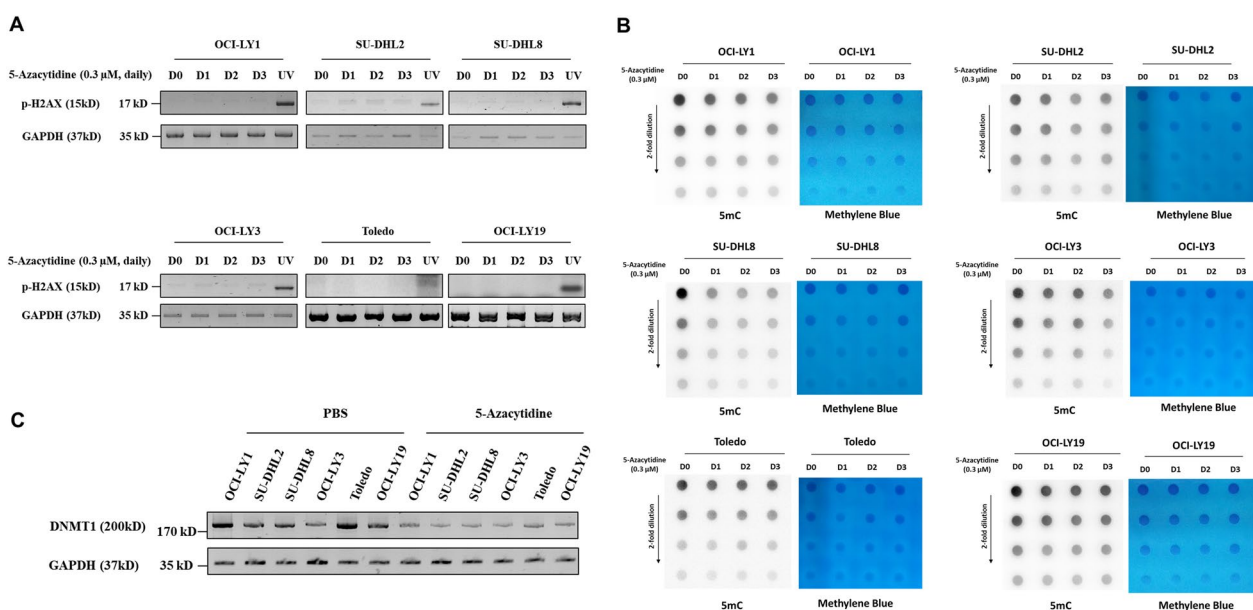
Fig. 2 Low-dose 5-azacytidine induces DNA demethylation without DNA damage. **A** Phospho-H2AX expression in the indicated DLBCL cell lines was detected using Western blotting; UV-treated cell was serving as positive control. **B** 5mC DNA dot blots showing the effect of low-dose 5-azacytidine on the global DNA methylation level for each cell line, and methylene blue served as the DNA loading control. **C** DNMT1 protein levels were detected using Western blotting in PBS or 5-azacytidine-treated cells

Liu *et al. Clinical Epigenetics*　　(2023) 15:75

Page 5 of 18

5-azacytidine induced DNA demethylation in all DLBCL cell lines without causing DNA damage.

5-Azacytidine induces transcriptome changes in DLBCL cell lines

Upon 5-azacytidine treatment, hierarchical clustering of the top variable gene expression profiles showed clustering by cell line and not by 5-azacytidine treatment, suggesting that 5-azacytidine did not have a dominant effect on the transcriptome (Fig. 3A). The effects on gene expression appeared to be divergent among the cell lines. The same non-dominant effect of 5-azacytidine on the transcriptome has also been reported in AML [23]. Consequently, to explore the expression profiles of genes that were related to both cisplatin sensitivity and 5-azacytidine treatment, we evaluated the differentially expressed genes (DEGs) between cisplatin-resistant DLBCL cell

lines and cisplatin-sensitive DLBCL cell lines with a conservative threshold with *p* values < 0.05, but not adjusted *p* values < 0.05 (Additional file 1: Fig. S3A). Additionally, we identified the DEGs between the PBS-treated group and the 5-azacytidine-treated group with *p* values < 0.5 (Additional file 1: Fig S3B). There were 2001 DEGs related to cisplatin sensitivity and 1092 DEGs associated with 5-azacytidine treatment. Among them, 122 genes were overlapping (Fig. 3B). Then, hierarchical clustering was performed using the expression profiles of the 122 genes, and the results identified two clusters. One cluster included OCI-LY1 cells treated with PBS, OCI-LY1 cells treated with 5-azacytidine, SU-DHL2 cells treated with PBS, and SU-DHL8 cells treated with PBS, suggesting unsatisfactory chemosensitization in OCI-LY1 cells (Fig. 3C). On the other hand, SU-DHL2 and SU-DHL8 cells that were treated with 5-azacytidine belonged to

Fig. 3 Low-dose 5-azacytidine treatment altered the expression of cisplatin sensitivity-related genes but did not have a dominant effect on the transcriptome. **A** Hierarchal clustering of the top variable gene expression profiles (interquartile range of probe sets between cell lines > 1). **B** Overlapping genes between the cisplatin sensitivity-related gene set and the 5-azacytidine treatment-regulated gene set. **C** The gene expression profiles of the 122 overlapping genes are shown using a heatmap

Liu *et al. Clinical Epigenetics*   (2023) 15:75

Page 6 of 18

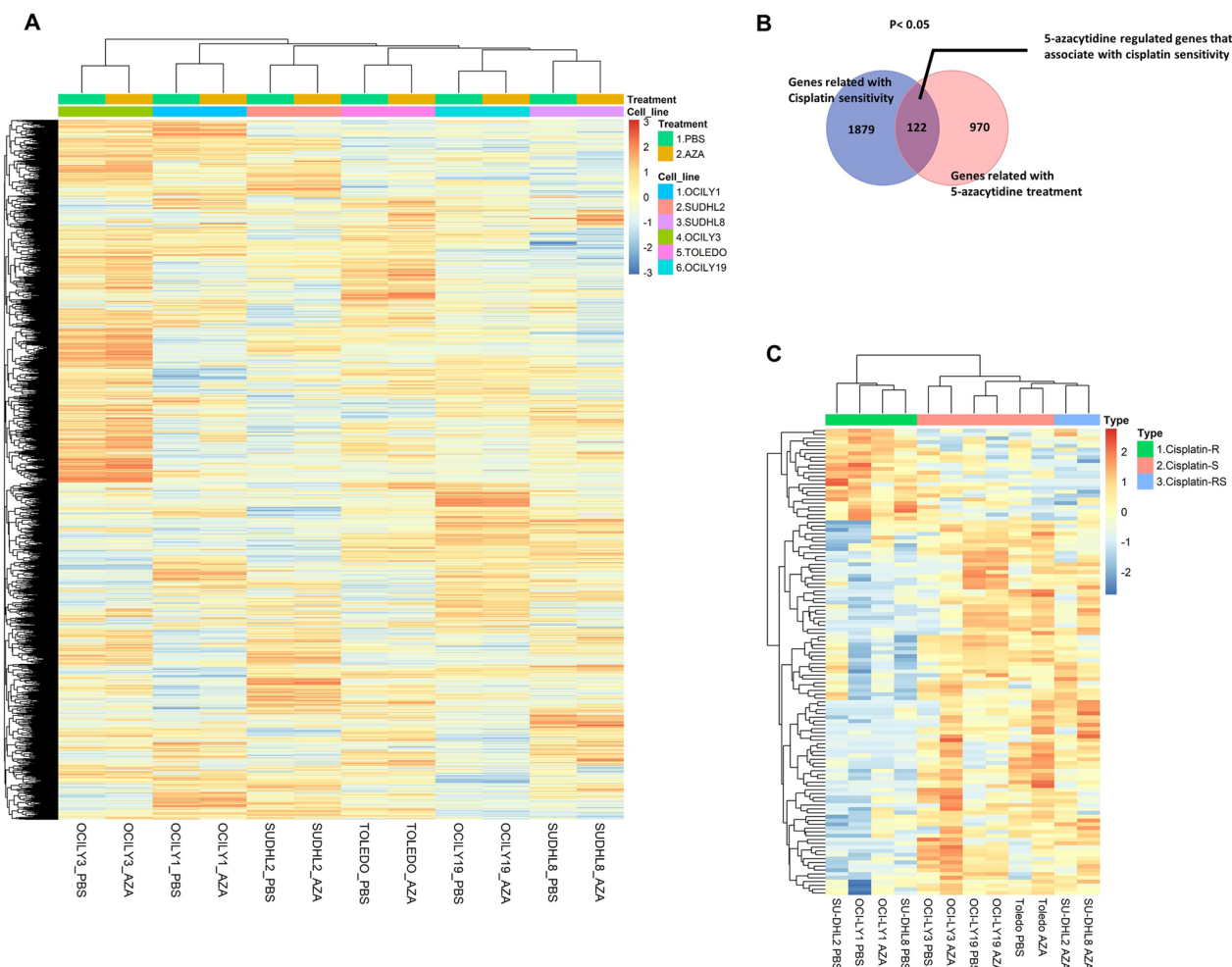the other cluster, which reflected satisfactory chemosensitization (Fig. 3C). These data suggested that low-dose 5-azacytidine treatment altered the expression of cisplatin sensitivity-related genes but did not have a dominant effect on the transcriptome.

5-Azacytidine treatment activates ERV expression in DLBCL cell lines

The differences in gene expression in each DLBCL cell line were subtle upon 5-azacytidine treatment, which may not be persuasive to explain the epigenetic priming effect of 5-azacytidine. Therefore, we explored the ERV activation profiles among various DLBCL cell lines. 5-Azacytidine can induce specific ERV transcripts in ovarian cancer [13, 24], melanoma [13], colorectal cancer [25], and endometrial cancer cells [26], thus activating the viral defense response. To analyze the genome-wide expression of human ERVs, we used an ERVmap pipeline that allowed for locus-specific genome-wide identification of proviral ERVs transcribed based on RNA-sequencing (RNAseq) data [27]. The open-source code of ERVmap and the accompanying web tool for quantifying ERVs in RNA-sequencing data are publicly available [27]. Comparison of the detectable transcribed ERVs revealed unique expression levels in each cell line (Fig. 4A). In all of the analyzed cell lines, we observed 23–35% of the ERVs at detectable levels (Fig. 4B). The count of total detectable ERV loci and sum of normalized ERV expression per cell line are shown in Fig. 4C and D. To identify ERVs induced by 5-azacytidine treatment, we excluded ERVs that were expressed in both the PBS- and 5-azacytidine-treated cell lines (Fig. 4E). Among all six cell lines, the SU-DHL8 had the greatest number of 5-azacytidine-induced ERV loci and the highest level of expression (Fig. 4F, G). In addition, the 5-azacytidine-induced ERV locus number and expressed level were correlated, suggesting that the expression of 5-azacytidine-induced ERVs was contributed by more different ERV loci but not by transcription of some loci at higher levels (Fig. 4H). To verify the ERVmap data, we selected four ERVs randomly, which from the results of a previous study [25]. These four ERVs were measured using qPCR. The ERV elements were significantly increased in SU-DHL8 cells after three consecutive days of 5-azacytidine

treatment, which was consistent with the ERVmap pipeline results (Fig. 4I–L).

5-Azacytidine-induced chemosensitization is mediated by the cGAS-STING axis

The activated ERV element forms dsRNA, after which dsRNA is detected by three signaling receptors: (1) toll-like receptor 3 (TLR3), which is located both on the cell membrane and in the endosomal membrane; (2) retinoic acid inducible gene I (RIG-I), which is located in the cytosol; and (3) melanoma differentiation associated gene 5 (MDA5), which is also located in the cytosol [28]. Activated dsRNA sensors showed increased RNA transcript and protein expression levels [13]. Therefore, to identify whether 5-azacytidine-induced ERVs activated dsRNA sensors, the protein and RNA levels of these three dsRNA sensors were detected using Western blot and normalized expression data based on RNA-sequencing data. Low-dose 5-azacytidine treatment activated MDA5 in the OCI-LY1, SU-DHL2, SU-DHL8, and OCI-LY3 cell lines but not in the Toledo and OCI-LY19 cell lines (Fig. 5A, B). This phenomenon was also shown in solid tumors such as colorectal and ovarian cancers. The very modest MDA5 activation in the Toledo cell line might be caused by the high level of ADAR1 (Additional file 1: Fig. S4). ADAR1 regulates dsRNA through adenosine-to-inosine editing and destabilization of RNA duplexes [29]. In OCI-LY19 cells, low-dose 5-azacytidine activated TLR3, as the RNA and protein expression levels increased (Fig. 5A) but not the cytosolic dsRNA sensors. RIG-I was not involved in 5-azacytidine-induced dsRNA recognition in any of the DLBCL cell lines (Fig. 5A, B). These data suggested that 5-azacytidine-induced dsRNA sensor activation might not account for the varying degrees of chemosensitizing effect in DLBCL cells.

The life cycle of ERV elements also entails the transient formation of RNA:DNA hybrids via using tRNAs as primers for reverse transcription [30]. Most ERVs are non-functional due to DNA recombination, mutations, and deletions. Some ERVs, however, especially proviral ERVs, contains polymerase (pol) with reverse transcriptase activity [13, 31, 32]. Cytosolic RNA:DNA hybrids can activate the cGAS-STING axis [33]. Therefore, to investigate cGAS-STING axis activation, we evaluated protein

(See figure on next page.)

Fig. 4 5-Azacytidine activates ERV expression in DLBCL cell lines. **A** ERV expression profiles are shown using a heatmap. **B** Histogram of the number of reads attributed to each of the 3220 ERV loci sorted in order of highest to lowest expressed ERVs for each cell line, *x*-axis: 3220 ERV loci in percentage scale, y-axis: scaled expression levels of ERVs in each cell line. **C** The total ERV locus number is shown using a bar chat. **D** The total ERV normalized expression is shown using a bar chat. **E** Venn diagram showing the number of baseline ERV, post-treatment ERV, and 5-azacytidine-induced ERV conditions in each cell line. **F** The number of 5-azacytidine-induced ERV loci in each cell line is shown using a bar chat. **G** The 5-azacytidine-induced ERV normalized expression level in each cell line is shown using a bar chat. **H** Correlation between the 5-azacytidine-induced ERV locus number and ERV expression. **I–L** The expression levels of several ERVs were detected using qPCR. **I–L** *p* < 0.05, **p* < 0.01 and ***p* < 0.001 (two-way ANOVA). AZA: 5-azacytidine
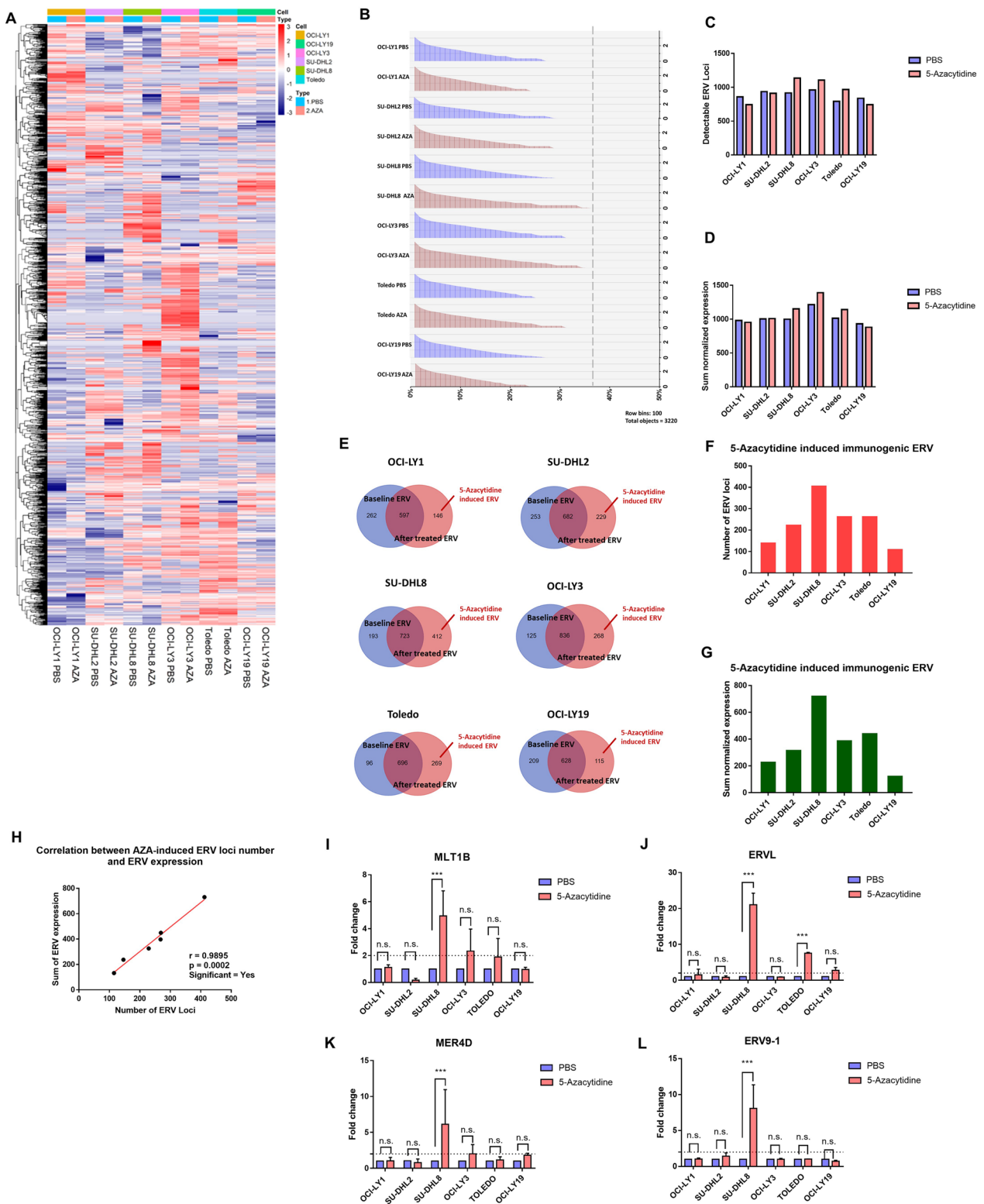
Liu *et al. Clinical Epigenetics*   (2023) 15:75

Page 7 of 18

Fig. 4 (See legend on previous page.)

Liu *et al. Clinical Epigenetics*   (2023) 15:75

Page 8 of 18

and RNA levels using western blotting and normalized RNAseq expression data, respectively. Among the cisplatin-resistant DLBCL cell lines, the double-stranded DNA (dsDNA) sensor cGAS was intrinsically highly expressed in SU-DHL8 cells, followed by SU-DHL2 cells, but was not expressed in OCI-LY1 cells (Fig. 5C, D). Activated cGAS synthesizes cGAMP that acts as an agonist of the endoplasmic reticulum-resident protein STING [34]. Among the cisplatin-resistant DLBCL cell lines, 5-azacytidine treatment significantly increased STING expression in the SU-DHL8 cell line, modestly increased expression in the SU-DHL2 cell line, and had no effect in the OCI-LY1 cell line (Fig. 5E, F). Here, we found that the cGAS-STING axis was closely related to cisplatin sensitivity in both intrinsic and 5-azacytidine-sensitized cell lines, except the OCI-LY3 cell line, suggesting that the mechanism related to cisplatin sensitivity in the OCI-LY3 cell line was cGAS-STING independent. We then explored the expression level of another dsDNA sensor, TLR9. Similar to cGAS, TLR9 can recognize RNA:DNA hybrids [35], and activating TLR9 has demonstrated potential as a novel immunotherapeutic approach to improve classic cancer therapies [36]. The TLR9 expression level was intrinsically high in OCI-LY3 cells and further increased after 5-azacytidine treatment (Fig. 5G, H). The STING and TLR9 activation patterns were significantly correlated with cisplatin sensitivity (Fig. 5I). In addition, the STING activation levels were consistent with the 5-azacytidine-induced cisplatin-sensitizing effects, despite the Pearson r value = 1 potentially due to the limited sample number (Fig. 5J).cGAMP-bound STING activates downstream kinases to activate the transcription factors IRF3 and NF-κB [37]. Therefore, we used the phospho-IRF3 level to identify IRF3 activation. For the NF-κB pathway, IKK and NF-κB p65 are phosphorylated and then translocation to the nucleus. Thus, IKK and NF-κB p65 have been reported to be early-response genes after 5-azacytidine treatment [14]. In this study, we treated the DLBCL cell lines for three consecutive days, so phospho-IKK and phospho-NF-κB p65 were not appropriate for detecting signaling activation. As an alternative, we used phospho-IκBα, which has been identified as a late-response gene after 5-azacytidine treatment, to monitor NF-κB signaling activation [14]. The phospho-IRF3 and phospho-IκBα levels showed that the IRF3 and NF-κB signaling pathways were significantly activated in SU-DHL8 cells and that the NF-κB signaling pathway was only slightly

activated in SU-DHL2 cells; however, neither the IRF3 nor NF-κB signaling pathway was activated in OCI-LY1 cells after 5-azacytidine treatment (Fig. 5K, L). Overall, in the DLBCL cell lines, the activation of intrinsic dsDNA sensors, including cGAS-STING and TLR9, was associated with cisplatin sensitivity. Low-dose 5-azacytidine could induce immunogenic ERV element transcription and formation of RNA:DNA hybrids recognized by intrinsic dsDNA sensors in DLBCL and thus activate the innate immune response. cGAS-STING axis activation was crucial to increasing the sensitivity to cisplatin treatment by 5-azacytidine priming.

cGAS-STING-mediated viral mimicry is dependent on reverse transcriptase activity

To verify whether the cGAS-STING mediated viral mimicry response was dependent on reverse transcriptase activity, we inhibited reverse transcriptase activity using delavirdine mesylate. Delavirdine mesylate is a non-nucleoside reverse transcriptase inhibitor that selectively inhibits reverse transcriptase and has low cellular cytotoxicity [38]. The reverse transcriptase activity assay showed that treatment with 50 μM of delavirdine mesylate one time and exposed for 3 days significantly repressed 5-azacytidine-induced reverse transcriptase activity in all three cell lines (Fig. 6A–C). Meanwhile, we found that the reverse transcriptase activity was increased after 5-azacytidine treatment in SU-DHL2 cells and SU-DHL8 cells, but no significant change was found in OCI-LY1 cells (Fig. 6A–C). In addition, reverse transcriptase inhibition abolished the 5-azacytidine priming-induced chemosensitizing effect in SU-DHL2 cells and SU-DHL8 cells as showed by cisplatin IC50 values (Fig. 6D, E, Additional file 1: Fig. S5B, C). The reverse transcriptase inhibition also abrogated STING and downstream IκBa activation in SU-DHL2 cells and blocked both IκBa and IRF3 activation in SU-DHL8 cells (Fig. 6G–I). However, in OCI-LY1 cells, reverse transcriptase inhibition neither showed influence on 5-azacytidine priming-induced chemosensitizing, nor on STING, IκBa and IRF3 activation (Fig. 6D, G and Additional file 1: Fig. S5A). To further investigate whether cGAS-STING was implicated in viral mimicry in DLBCL, we knocked down cGAS and STING using siRNAs in SU-DHL8 cells. Then, by detecting the expression levels of cGAS and STING with and without 5-azacytidine treatment in the negative control and knockdown cell lines, we found

(See figure on next page.)

Fig. 5 5-Azacytidine induces chemosensitization mediated by the cGAS-STING axis. **A**–**H** The expression levels of target proteins were measured using Western blotting and RNA-sequencing data. MDA5, RIG-I, cGAS, and STING are encoded by the IFIH1, DDX58, MB21D1, and TMEM173 genes, respectively. **I** Pearson correlation between the dsDNA sensor activation level and cisplatin sensitivity. **J** Pearson correlation between cGAS-STING activation and the chemosensitization effect. **K**, **L** The expression and phosphorylation levels of IRF3 and IκBα were measured using western blotting
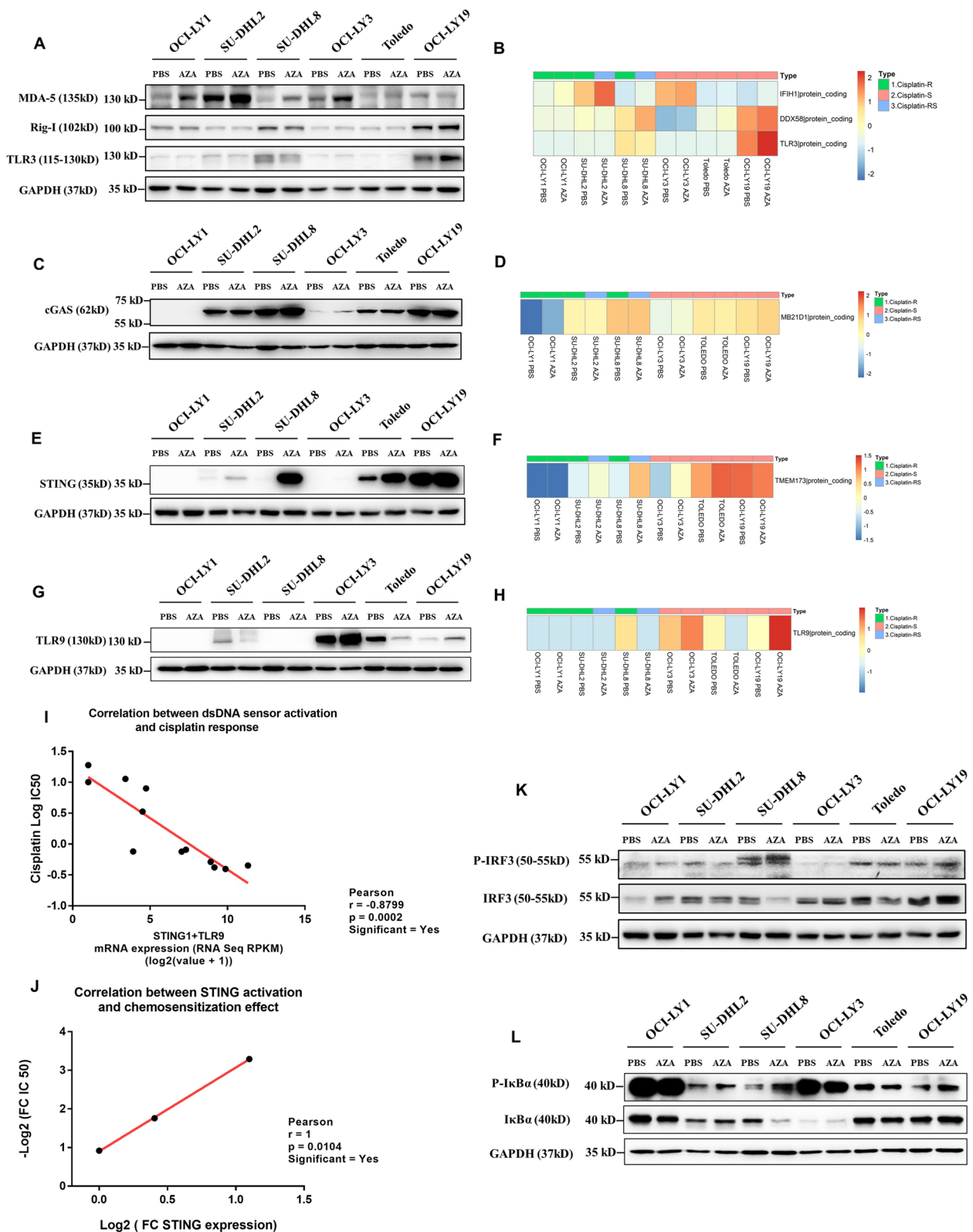
Liu *et al. Clinical Epigenetics*   (2023) 15:75

Page 9 of 18

Fig. 5 (See legend on previous page.)

Liu *et al. Clinical Epigenetics*   (2023) 15:75

Page 10 of 18

that both cGAS and STING siRNAs had good knockdown effects on their target genes (Fig. 6J). Knockdown cGAS blocked 5-azacytidine-induced STING upregulation (Fig. 6J). Next, we measured downstream IκBa and IRF3 activation and found that both cGAS and STING knockdown could abrogate downstream signal activation (Fig. 6K–L). Taken together, these data suggested that cGAS-STING was implicated in viral mimicry cytosolic sensing in DLBCL and was dependent on reverse transcriptase activity. Except for the proviral ERVs, long interspersed nuclear elements (LINEs) may also be one contributor to the reverse transcriptase activity. Therefore, we analyzed the LINEs expression using TElocal which is a tool utilizes both uniquely and ambiguously mapped reads to quantify transposable element expression at the locus level. As shown in Additional file 1: Fig. S6, among the three cisplatin-resistant DLBCL cell lines, an increase LINEs expression was found on OCI-LY1, and a slight increase was found on SU-DHL2 after 5-azacytidine treatment. However, the LINE expression did not increase on SU-DHL8, while it decreased after 5-azacytidine treatment (Additional file 1: Fig. S6), suggesting 5-azacytidine-induced ERVs expression was the main contributor to the reverse transcriptase activity.

A combination of vitamin C and 5-azacytidine could be a potential remedy for insufficient epigenetic priming

Combining vitamin C and 5-azacytidine can enhance immune signals, including increasing expression of bidirectionally transcribed ERV transcripts, increasing cytosolic dsRNA levels, and activating the IFN-inducing cellular response [39]. This synergistic effect is likely the result of both passive DNA demethylation by 5-azacytidine and active conversion of 5mC to 5-hydroxymethylcytosine (5hmC) by ten-eleven translocation (TET) enzymes at long terminal repeat (LTR) regions of ERVs because vitamin C acts as a cofactor for TET proteins [39]. To overcome the insufficient epigenetic priming on OCI-LY1 and further improve the effect of epigenetic priming on SU-DHL2, a combination of three consecutive days of low-dose (0.3 μM) 5-azacytidine treatment and three days of 250 μM vitamin C administration was applied. The combination of 5-azacytidine and vitamin C further improved cisplatin sensitivity in SU-DHL2 cells but not in OCI-LY1 cells (Fig. 7A, Additional file 1: Fig.

S7A, B). In addition, the combination treatment activated STING expression in SU-DHL2 cells but not in OCI-LY1 cells (Fig. 7B). Consistent with these in vitro data, in OCI-LY1 xenograft models, the combination of 5-azacytidine and vitamin C exhibited limited benefit in enhancing cisplatin sensitization (Additional file 1: Fig. S7C–E). In a previous study, we showed that GLUT3, a major transporter of the oxidized form vitamin C, is essential to vitamin C treatment efficiency [40]. Therefore, we detected the GLUT3 expression levels in OCI-LY1 and SU-DHL2 cells (Fig. 7C). Although both OCI-LY1 and SU-DHL2 cells had low SLC2A3 (gene encoding GLUT3) mRNA levels, SU-DHL2 cells showed higher GLUT3 protein expression than OCI-LY1 cells (Fig. 7D). Vitamin C acts as a cofactor of TET2; however, the TET2 mRNA level was lower in OCI-LY1 cells than in other DLBCL cell lines (Additional file 1: Fig. S7F), which also might be one of the reasons for the low efficacy of vitamin C in OCI-LY1 cells. To further verify the effect of the vitamin C and 5-azacytidine combination treatment, we transduced OCI-LY1 cells with a GLUT3-overexpressing lentivirus or empty vector lentivirus (Fig. 7E). Epigenetic priming using a combination of vitamin C and 5-azacytidine significantly improved the cisplatin-sensitizing effect (Fig. 7F). It was worth noting that in the SLC2A3-overexpressing OCI-LY1cell line, the IC50 of cisplatin dropped below the clinically achievable dose after combination epigenetic priming (Fig. 7F). Moreover, STING expression was activated after combination epigenetic priming in the SLC2A3-overexpressing OCI-LY1cell line (Fig. 7G). Consistent with the in vitro data, in SLC2A3-overexpressing OCI-LY1 xenograft models, the combination of 5-azacytidine and vitamin C significantly improved the tumor-suppressive effect of cisplatin compared with that in empty vector-transduced OCI-LY1 xenograft models (Fig. 7H–J). These data suggested that vitamin C could be a solution to address insufficient epigenetic priming and that GLUT3 was indispensable in this remedy.

Discussion

Epigenetic priming-induced chemosensitization is a potential solution for the unmet needs of salvage chemotherapy. However, its potential and mechanism for improving outcomes in relapsed/refractory DLBCL

(See figure on next page.)

Fig. 6 cGAS-STING-mediated viral mimicry was dependent on reverse transcriptase activity. **A**–**C** Reverse transcriptase activity was measured after PBS, AZA, RTi, and AZA + RTi treatment on OCI-LY1, SU-DHL2, and SU-DHL8, respectively. **D**–**F** IC50 values were calculated using cell viability measured on day 5 after pretreatment with PBS, AZA, RTi, and the AZA + RTi combination on OCI-LY1, SU-DHL2, and SU-DHL8, respectively. **G**–**I** The expression of cGAS and STING and phosphorylation levels of IRF3 and IκBα were measured using western blotting after PBS, AZA, RTi, and AZA + RTi treatment on OCI-LY1, SU-DHL2, and SU-DHL8, respectively. **J**–**L** The expression of cGAS and STING and phosphorylation levels of IRF3 and IκBα were measured in the negative control and knockdown cell lines with and without 5-azacytidine treatment on SU-DHL8 cells. **A** and **B** *$p < 0.05$, **$p < 0.01$ and ***$p < 0.001$ (two-way ANOVA). AZA: 5-azacytidine, RTi: reverse transcriptase inhibitor (delavirdine mesylate)

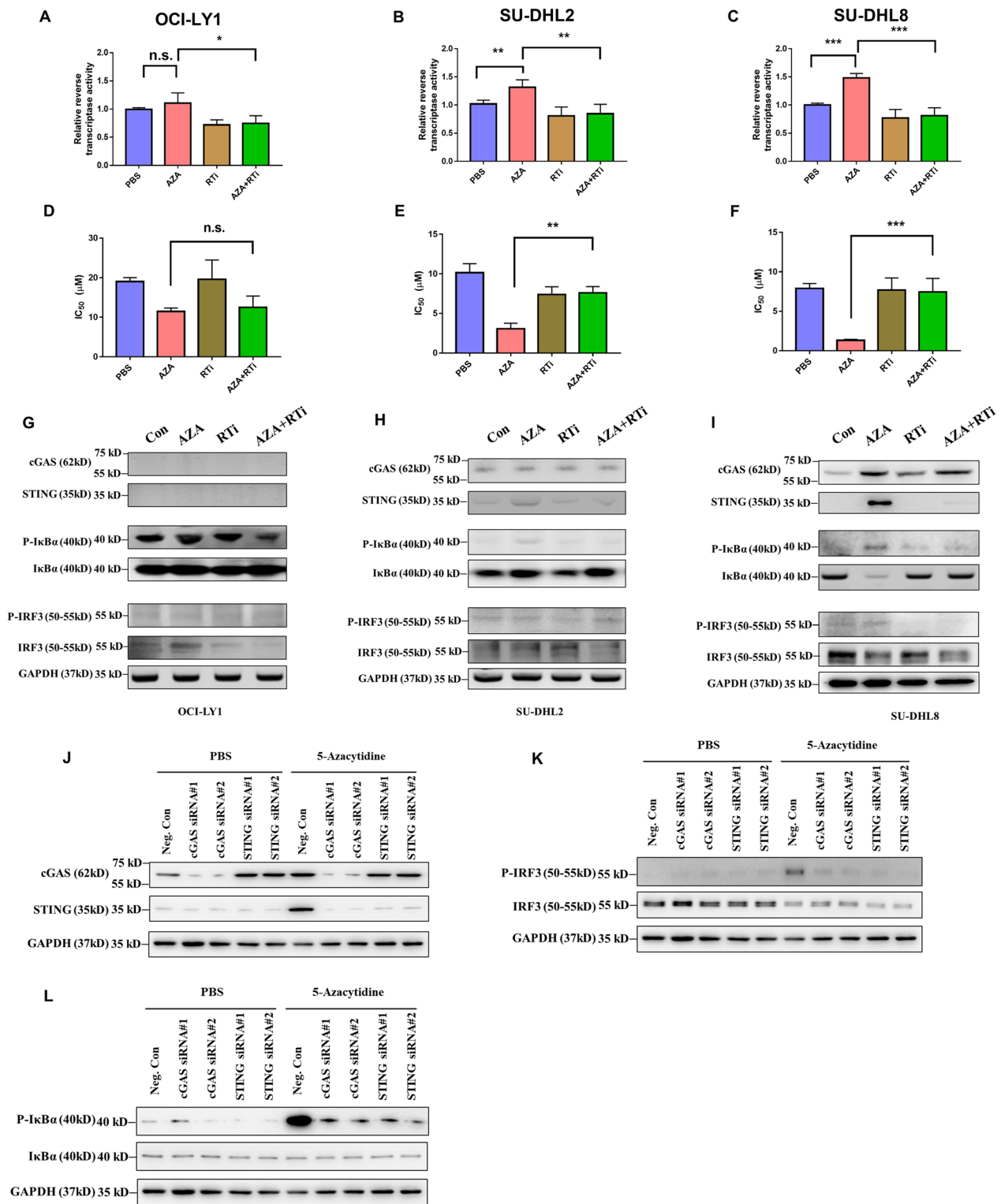Liu *et al. Clinical Epigenetics*   (2023) 15:75

Page 11 of 18

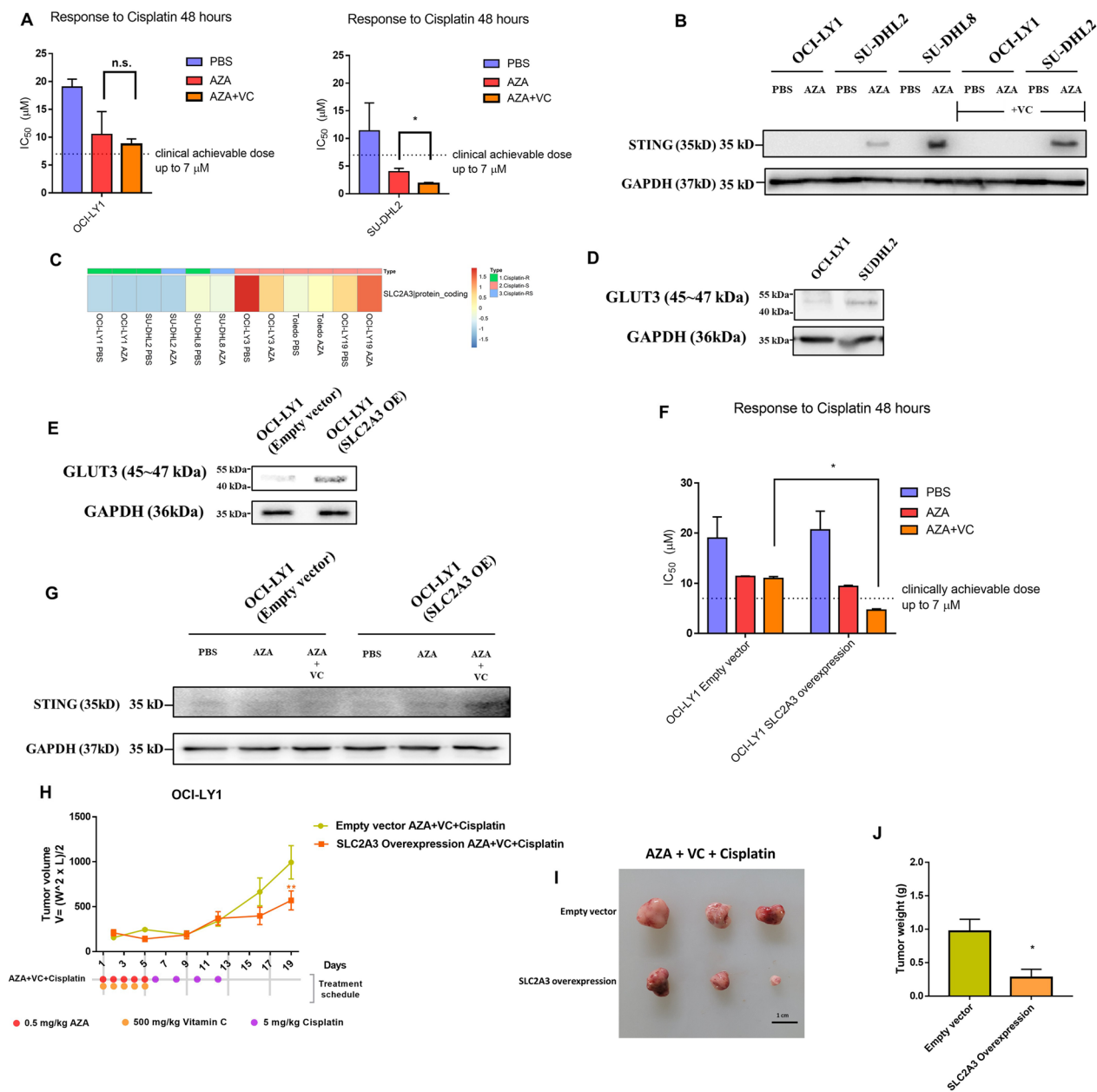**Fig. 6** (See legend on previous page.)

Fig. 7 A combination of vitamin C and 5-azacytidine could be a potential remedy for insufficient epigenetic priming. **A** IC50 values were calculated using cell viability measured on day 5. *$p < 0.05$, **$p < 0.01$ and ***$p < 0.001$ (two-way ANOVA). **B**, STING expression levels were measured using western blotting. **C**, **D** GLUT3 expression levels were measured using RNA-sequencing data and western blotting, GLUT3 is encoded by the SLC2A3 gene. **E** GLUT3 expression levels were measured using western blotting of empty vector-expressing and SLC2A3-overexpressing OCI-LY1 cell lines, OE: overexpression. **F** IC50 values were calculated using cell viability measured on day 5. *$p < 0.05$, **$p < 0.01$ and ***$p < 0.001$ (two-way ANOVA). **G** STING expression levels were measured using western blotting. **H**–**J** Subcutaneous tumor sizes, xenograft tumor images, and tumor weights of xenografts from empty vector-expressing or SLC2A3-overexpressing OCI-LY1 tumor-bearing models are shown. *$p < 0.05$, **$p < 0.01$ and ***$p < 0.001$ (*t* test). AZA: 5-azacytidine, VC: vitamin C, OE: overexpression

are unknown (Additional file 1: Fig. S8). In the current study, we showed that 5-azacytidine epigenetic priming improved platinum-based salvage chemotherapy in DLBCL via ERV-induced cGAS-STING activation rather than via dsRNA sensor activation. In addition,

heterogeneous cGAS/STING expression was observed in DLBCL patients, and the cGAS/STING deficiency could impair the chemosensitizing effect (Fig. 8A). Vitamin C showed the potential to improve insufficient epigenetic priming, and this effect was dependent on the GLUT3
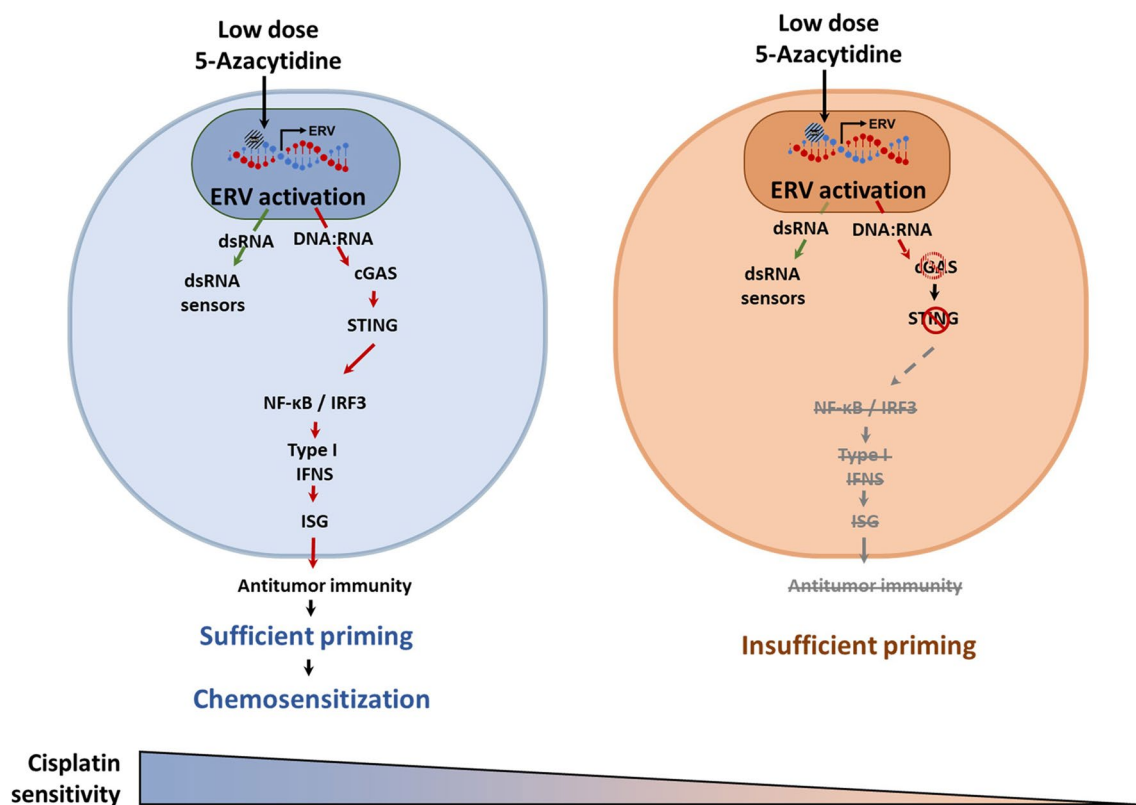
Cancer type: diffuse large B-cell lymphoma (DLBCL)

Fig. 8 Epigenetic priming-induced chemosensitization is a potential solution for the unmet needs of salvage chemotherapy. 5-azacytidine epigenetic priming improved platinum-based salvage chemotherapy in DLBCL via ERV-induced cGAS-STING activation rather than via dsRNA sensor activation, cGAS-STING activation is likely involved over dsRNA detection due to the putatively high levels of reverse transcriptase in DLBCL cells, and the cGAS/STING deficiency could impair the chemosensitizing effect

level (Fig. 8B). Although there are still difficulties to be overcome, our study suggested that the effectiveness of epigenetic priming would increase the efficacy of salvage chemotherapy in patients with DLBCL.

This study aimed to elucidate the effect of 5-azacytidine as a chemosensitizer in a cisplatin-containing salvage regimen and demonstrate the mechanism to help explain further clinical data.

By comparing cisplatin sensitivity in DLBCL cell lines with or without 5-azacytidine pretreatment, we concluded that 5-azacytidine had efficacy as a chemosensitizer in a cisplatin-containing salvage regimen. However, the degree of benefit varied among the cells. Different degrees of sensitization indicated a complicated mechanism of action. Several clinical studies have reported that 5-azacytidine shows a chemosensitizing effect in newly diagnosed or relapsed/refractory DLBCL, but not all patients receive the same benefit [11, 41]. Therefore, it is essential to demonstrate the

mechanism and develop a mechanism-based method to predict the chemosensitizing effect.

In this study, we found that both dsRNA sensors, including MDA5 and TLR3, and dsDNA sensors, including cGAS and TLR9, were activated by 5-azacytidine treatment, although the degree of activation of each sensor in each cell line differed (Fig. 5A–H). Our data suggest that dsDNA sensors, especially cGAS-STING axis, are critical contributors to the chemosensitizing function of 5-azacytidine. Finally, we assessed the activation status of the cGAS-STING downstream transcription factors IRF3 and NF-κB and confirmed that epigenetic priming using 5-azacytidine potentially improved cisplatin sensitivity. The mechanism of action was attributed to ERV-induced cGAS-STING activation, and cancer cell-intrinsic cGAS expression levels showed the potential to predict chemosensitization, which delineates a strategy for salvage chemotherapy.

Heterogeneous expression levels of cGAS and STING were observed in DLBCL patients (Additional file 1: Fig. S9A, B), and deficiency of cGAS in DLBCL cells impaired the chemosensitizing effect and caused insufficient epigenetic priming in cisplatin resistant cells. Here we tried to propose a concept to stratify DLBCL patients (Additional file 1: Fig. S9C); however, this prediction method still needs optimization, such as machine learning base on multi-omics data and validation.

Vitamin C showed the potential to improve insufficient epigenetic priming, and this effect was dependent on the GLUT3 level. However, the detailed mechanism about how STING being upregulated by vitamin C if cGAS is not detecting the transcribed repetitive elements still needs a further study. Here we speculated that the combination of 5-azacytidine and vitamin C could activate a positive feedback loop between IRF9 and STING (Additional file 1: Fig. S10). A previous report showed that IRF9 can be induced by decitabine and TET2-catalytic domain [42], so there is a large possibility that IRF9 could also be induced by 5-azacytidine and vitamin C combination treatment. In addition, a positive feedback loop between IFR9 and STING has also been reported by Ma et al. [43]. So, this positive feedback loop may activate STING independent of cGAS.

In a previous study, Liu et al. [39] showed synergistic effects mediating inhibition of cancer cell proliferation and increased apoptosis between physiological levels of vitamin C and decitabine. Therefore, insufficient epigenetic priming could be addressed with physiological levels of vitamin C if overcome GLUT3 deficiency. For example, AICAR (an AMPK activator, in phase 3 trials) has shown potential to pharmacologically activate GLUT3 expression [44]. AICAR was also shown to mediate protection against cisplatin-induced acute kidney injury [45]. Here, although we did not explore the effect of AICAR, it may shed new light on 5-azacytidine-induced epigenetic priming in salvage chemotherapy in DLBCL.

Conclusion
In conclusion, epigenetic priming using 5-azacytidine could potentially improve cisplatin chemosensitivity in cisplatin-resistant DLBCL cell lines. The cGAS-STING pathway was the critical contributor to resensitization. Our ongoing phase II trial (NCT03719989) with parallel biomarker analysis will reveal whether the results we obtained in this preclinical work are translatable to the clinic and can be applied in the future.

Methods
Cell lines
The DLBCL cell line OCI-LY1 was cultured in Iscove's modified Dulbecco's medium (IMDM; Gibco, Grand Island, NY, USA) supplemented with 20% fetal bovine serum (FBS; Gibco, Grand Island, NY, USA) and 1% penicillin–streptomycin (Gibco, Grand Island, NY, USA) at 37 °C and 5% CO_2. The DLBCL cell line OCI-LY19 was cultured in alpha-MEM supplemented with 20% FBS and 1% penicillin–streptomycin (Gibco, Grand Island, NY, USA) at 37 °C and 5% CO_2. The DLBCL cell lines SU-DHL8 and OCI-LY3 were cultured in RPMI 1640 medium (WELGENE, Seoul, Republic of Korea) supplemented with 20% FBS and 1% penicillin–streptomycin at 37 °C and 5% CO_2. The DLBCL cell lines SU-DHL2 and Toledo were cultured in RPMI 1640 medium supplemented with 20% FBS and 1% penicillin–streptomycin at 37 °C and 5% CO_2. The cell lines were obtained from the American Type Culture Collection and DMSZ. STR analysis was conducted after sampling for authentication. All DLBCL cell lines used in this study were Epstein–Barr virus (EBV) negative.

GLUT3-overexpressing cell line
A lentiviral vector for GLUT3 overexpression (lentiviral ORF clone of SLC2A3, mGFP tagged, CAT#: RC204430L4) and an empty vector (pLenti-C-mGFP-P2A-Puro Lentiviral Gene Expression Vector, CAT#: PS100093) were purchased from Origene. The overexpression vector or empty vector was cotransfected into H293T cells with pRSV-REV (Addgene #12253), pMDLg/pRRE (Addgene #12251), and pMD2.G (Addgene #12259) using Lipofectamine 3000 reagent (Thermo Fisher, Waltham, MA USA). Viral particles were harvested using a Lenti-X Concentrator (Takara, Kusatsu, Shiga, Japan) after two days of culture. Transduction with lentiviral particles was performed according to the multiplicity of infection (MOI) of OCI-LY1 cells. Positively infected cells were sorted using fluorescence-activated cell sorting (FACS; BD FACSAria III).

DLBCL xenograft models
We purchased 6- to 8-week-old female athymic nude mice from The Jackson Laboratory. Mouse studies were performed in specific pathogen-free (SPF) facilities with approval of the Institutional Animal Care and Use Committee (IACUC) of Seoul National University (IACUC approval number: SNU-210609-3). OCI-LY1, SU-DHL2, empty vector-expressing OCI-LY1, or SLC2A3-overexpressing OCI-LY1 cells were subcutaneously injected into the back of athymic nude mice. A total of 5×10^6 cells in 100 μL 1:1 PBS/high-concentration Matrigel (Corning,

Liu *et al. Clinical Epigenetics*   (2023) 15:75

Page 15 of 18

Glendale, AZ, USA) solution were injected. Tumor length and width were measured twice a week with calipers. Tumor volumes were calculated as $(width^2 \times length)/2$. On day 20, all mice were sacrificed, and the tumor xenografts were collected for imaging and weighing.

In vivo 5-azacytidine epigenetic priming and cisplatin treatment

The 5-azacytidine (A1287, Sigma-Aldrich, Saint Louis, MO, USA) was dissolved in warm DMSO (Sigma-Aldrich, Saint Louis, MO, USA) to make a stock solution. The injection solution was freshly prepared before each use by diluting the stock solution with PBS and passing it through a 0.22-μm filter for sterilization. Mice were randomly grouped into 5-azacytidine treatment group and no treatment group and then received an intraperitoneal injection of 0.5 mg/kg 5-azacytidine in PBS for five consecutive days, starting on day 1 after the development of tumors with a volume of approximately 150–200 mm^3, while the no-treatment group received the same volume of PBS administered intraperitoneally.

Mice received an intraperitoneal injection of 5 mg/kg cisplatin in PBS four times every two days, starting on day 6 after 5-azacytidine epigenetic priming.

Simulation of cisplatin pharmacokinetics

The plasma levels of cisplatin in human patients following administration of an 80 mg/m^2 dose, the highest single dose recommended in the drug product label, via intravenous injection have been reported previously [22]. At a specific time point, T_{max} and $T_{1/2}$ were determined according to a widely accepted procedure [22]. The physiologically based pharmacokinetic (PBPK) model-predicted value was determined using typical physiological and biochemical parameters with PKQuest [46]. Predicted pharmacokinetic curves were compared with existing reports to ensure accuracy [47]. The clinically achievable dose was determined according to the plasma cisplatin concentration after $T_{1/2}$.

In vitro azacytidine epigenetic priming

DLBCL cell lines were seeded in T75 flasks, cultured for 24 h, and then exposed to 0.3 μM 5-azacytidine for three consecutive days. 5-Azacytidine was added to the culture medium daily.

Cell viability assay

DLBCL cell lines were seeded in 96-well plates, cultured for 24 h and then exposed to increasing doses of cisplatin for 48 h, as described previously [40]. Next, 10 μL Cell Counting Kit 8 (CCK8) reagent (Dojindo, Japan) was added to each well and incubated for 4 h. Then, the optical density (OD) values were measured at 450 nm with a microplate reader.

Western blot analysis

Whole-cell lysates were collected using Kinexus protein lysis buffer [containing 20 mM MOPS (pH 7.0), 2 mM EGTA, 5 mM EDTA, 30 mM sodium fluoride, 60 mM β-glycerophosphate (pH 7.2), 20 mM sodium pyrophosphate, 1 mM sodium orthovanadate, 1% Triton X-100, 1 mM PMSF, 30 μL/mL phosphatase inhibitor cocktail, and 1 g/mL protein inhibitor cocktail (Hoffmann-La Roche, Ltd., Switzerland)], as described previously [48]. The cell lysates were separated on 8–15% SDS–PAGE gels and transferred to nitrocellulose membranes, which were blocked, washed, and incubated overnight at 4 °C with appropriate primary antibodies. After washing, the membranes were incubated with an appropriate HRP-conjugated secondary antibody, and enhanced chemiluminescence (ECL) was used to visualize the blots. The antibodies used in this study are listed in Additional file 1: Table S1.

Dot blot analysis

DNA samples were isolated using a QIAamp DNA Micro Kit (Cat# 51306, QIAGEN, Hilden, Germany) as described previously [40]. The isolated DNA was denatured, and twofold serial dilutions were spotted onto a nitrocellulose membrane in an assembled Bio-Dot apparatus (Bio–Rad, Hercules, California, USA). After drying, blocking, and washing (1 × Tris Buffered Saline, with 0.1% Tween 20), the membranes were incubated overnight at 4 °C with appropriate primary antibodies. Then, an HRP-conjugated secondary antibody was added to the membranes and incubated for 1 h, and ECL was used to visualize the blots. In addition, another membrane was stained with 0.02% methylene blue in 0.3 M sodium acetate (pH 5.2) to visualize the DNA as a total genomic DNA loading control.

RNA isolation

Total RNA was isolated using TRIzol reagent (Invitrogen). RNA quality was assessed with an Agilent 2100 bioanalyzer (Agilent Technologies, Amstelveen, The Netherlands), and RNA quantification was performed using an ND-2000 Spectrophotometer (Thermo Inc., DE, USA).

Quantitative real-time PCR (qPCR)

The expression of ERV elements was measured using qPCR as described previously [48]. GAPDH mRNA expression served as the internal control. The assay was conducted using Bioneer SYBR Green qPCR Premix and an Applied Biosystems 7500 PCR instrument. Total RNA

Liu *et al. Clinical Epigenetics*   (2023) 15:75

Page 16 of 18

was isolated with TRIzol reagent, and 2.5 ng total RNA was used to produce cDNA from the isolated RNA with cDNA EcoDry Premix (Takara, Kusatsu, Shiga, Japan) according to the manufacturer's instructions. The primer sequences used in this study are listed in Additional file 1: Table S2.

Knockdown of cGAS (encoded by MB21D1) and STING (encoded by TMEM173) expression by RNA interference (RNAi)

SU-DHL8 cells were transfected with a set of small interfering RNAs (siRNAs) targeting MB21D1, TMEM173, or a non-targeting control siRNA. Transfections were conducted using electroporation with the LONZA SF kit DC-100 program (LONZA, Basel, Switzerland) and 4D X-units. The siRNA sequences used in this study are shown in Additional file 1: Table S3.

Reverse transcriptase assay

The reverse transcriptase assay was performed according to the user manual supplied with the EnzChek Reverse Transcriptase Assay Kit (E22064, Thermo Fisher, Waltham, MA USA). Equivalent concentrations of whole-cell lysates were assayed, and the fluorescence was measured at an excitation wavelength of 480 nm and emission wavelength of 520 nm.

RNAseq library preparation and sequencing

Libraries were prepared from total RNA using a NEBNext Ultra II Directional RNA-Seq Kit (NEW ENGLAND Bio-Labs, Inc., UK). mRNA isolation was performed using a Poly(A) RNA Selection Kit (LEXOGEN, Inc., Austria). The isolated mRNAs were used for cDNA synthesis and shearing following the manufacturer's instructions. Indexing was performed using the Illumina indexes. An enrichment step was carried out using PCR. Subsequently, the libraries were checked using an Agilent 2100 bioanalyzer (DNA High Sensitivity Kit) to evaluate the mean fragment size. Quantification was performed using a library quantification kit and StepOne Real-Time PCR System (Life Technologies, Inc., USA). High-throughput sequencing was performed as paired-end 100-bp sequencing using a NovaSeq 6000 (Illumina, Inc., USA).

RNAseq data analysis

Cellular gene expression and proviral ERV locus expression were determined using the ERVmap pipeline [27]. The code is available on GitHub and via a web-based tool on https://www.ervmap.com. Data mining and graphic

visualization were performed using the R (version 4.0.5, www.r-project.org) and Bioconductor packages [49].

Accession number

Expression data from DLBCL cell lines have been deposited in the Gene Expression Omnibus and are accessible under accession number GSE190319.

Statistical analysis

Data are presented as the mean ± standard error of the mean (SEM). All experiment groups contained at least three biological replications or technical replications to ensure adequate power to detect a pre-specified effect size. The samples from each group were compared by Student's *t* test, and multiple comparisons among groups were performed using analysis of variance (ANOVA) with the GraphPad Prism program 7.00.

Abbreviations

5hmC	5-Hydroxymethylcytosine
5mC	5-Methylcytosine
AML	Acute myeloid leukemia
ANOVA	Analysis of variance
ASCT	Autologous stem cell transplantation
CAR-T	Chimeric antigen T-cell
CCK8	Cell Counting Kit 8
CTAs	Cancer–testis antigens
DEGs	Differentially expressed genes
DLBCL	Diffuse large B-cell lymphoma
DNMTi	DNA methyltransferases inhibitor
DNMTs	DNA methyltransferases
dsDNA	Double-stranded DNA
dsRNA	Double-stranded RNA
EBV	Epstein–Barr virus
ECL	Enhanced chemiluminescence
ERV	Endogenous retrovirus
IACUC	Institutional Animal Care and Use Committee
IFN	Interferon
LINE	Long interspersed nuclear element
LTR	Long terminal repeat
MDA5	Melanoma differentiation-associated gene 5
MDS	Myelodysplastic syndrome
NHL	Non-Hodgkin lymphoma
OD	Optical density
PBPK	Physiologically based pharmacokinetic
pol	Polymerase
pola-BR	Polatuzumab vedotin combination with bendamustine and rituximab
R-CHOP	Rituximab, cyclophosphamide, doxorubicin, vincristine, and prednisone
R-GDP	Rituximab, gemcitabine, dexamethasone, and cisplatin
RIG-I	Retinoic acid-inducible gene I
RNAseq	RNA sequencing
SEM	Standard error of the mean
siRNAs	Small interfering RNAs
SPF	Specific pathogen-free
TET	Ten-eleven translocation
TLR3	Toll-like receptor 3
TSGs	Tumor suppressor genes

Liu *et al. Clinical Epigenetics*   (2023) 15:75

Page 17 of 18

Supplementary Information

The online version contains supplementary material available at https://doi.org/10.1186/s13148-023-01493-x.

Additional file 1: Figure S1. A-B. Schematics of the in vitro and in vivo treatment regimens, respectively. **Figure S2**. A-F. Six DLBCL cell lines were exposed to 5-azacytidine (0.3 μM) or PBS for three consecutive days followed by treatment with different doses of cisplatin for 48 hours. Cell viability measured on day 5 (normalized to that on day 3 for AZA- or PBS-treated cells) is shown. **Figure S3**. A, Gene expression profiles between the cisplatin-sensitive group and cisplatin-resistant group are shown using a heatmap. R: Resistant, S: Sensitive, RS: Re-sensitization. B, Gene expression profiles without or with 5-azacytidine treatment are shown using a heatmap. **Figure S4**. The expression level of ADAR1 determined using western blotting and RNAseq-based normalized expression data. **Figure S5**. Cell viability assay, OCI-LY1, SU-DHL2 and SU-DHL8 cells were treated with PBS, AZA, RTi, and AZA+RTi, followed by treatment with different doses of cisplatin for 48 hours. AZA: 5-azacytidine, RTi: reverse transcriptase inhibitor (delavirdine mesylate). **Figure S6**. The LINEs expression levels in each cell lines treated with PBS or 5-azacytidine were shown using a bar chat. **Figure S7**.   A-B. OCI-LY1 and SU-DHL2 cells were treated with 0.3 μM 5-azacytidine for three consecutive days and 250 μM vitamin C once exposed for three days or only 0.3 μM 5-azacytidine or PBS for three consecutive days, followed by treatment with different doses of cisplatin for 48 hours. C-E, Subcutaneous tumor sizes, xenograft tumor images and tumor weights of xenografts from OCI-LY1 tumor-bearing models are shown. *$p < 0.05$, *$p < 0.01$ and ***$p < 0.001$ two-way ANOVA). F. The expression level of TET2 determined using RNAseq-based normalized expression data is shown in a heatmap. **Figure S8**. Schematic diagram showed the background of the current study. Epigenetic priming-induced chemosensitization is a potential solution for the unmet needs of salvage chemotherapy, however, its potential and mechanism to improve outcomes in relapsed/refractory DLBCL is unknow. **Figure S9**. (A-B) MB21D1 and TMEM173, encoded cGAS and STING respectively, normalized expression level in 37 DLBCL patients (TCGA, PanCancer Atlas), (C) Concept schematic diagram to stratify DLBCL patients according to cGAS/STING expression level. The dots represent TCGA DLBCL patients' cGAS and STING expression levels. **Figure S10**. Vitamin C showed the potential to improve insufficient epigenetic priming, and this effect was dependent on the GLUT3 level. **Table S1**. Antibodies. **Table S2**. RT–qPCR primer sequences. **Table S3**. siRNA sequences.

Author contributions

Conception and design were performed by JH and JL; development of methodology by JL and SM; acquisition of data by JL and SM; analysis and interpretation of data by JL; writing, review, and/or revision of the manuscript by JL, TK-K, and JH; administrative, technical, or material support by SM; study supervision by JH, YK, DY-S, JM-B, and SS-Y; research by JL, JP, SM, DK, and EP. All authors read and approved the final manuscript.

Availability of data and materials

The RNA-seq and MBD-seq datasets generated and/or analyzed during the current study are available in the [Gene Expression Omnibus, GSE190321] repository.

Declarations

Ethics approval and consent to participate

Mouse studies were performed in specific pathogen-free (SPF) facilities with approval of the Institutional Animal Care and Use Committee (IACUC) of Seoul National University (IACUC approval number: SNU-210609-3).

Competing interests

The authors declare no competing interests.

References

1. Armitage JO, Weisenburger DD. New approach to classifying non-Hodgkin's lymphomas: clinical features of the major histologic subtypes. Non-Hodgkin's lymphoma classification project. J Clin Oncol. 1998;16(8):2780–95.
2. Feugier P, Van Hoof A, Sebban C, Solal-Celigny P, Bouabdallah R, Ferme C, et al. Long-term results of the R-CHOP study in the treatment of elderly patients with diffuse large B-cell lymphoma: a study by the Groupe d'Etude des Lymphomes de l'Adulte. J Clin Oncol. 2005;23(18):4117–26.
3. Crump M, Neelapu SS, Farooq U, Van Den Neste E, Kuruvilla J, Westin J, et al. Outcomes in refractory diffuse large B-cell lymphoma: results from the international SCHOLAR-1 study. Blood. 2017;130(16):1800–8.
4. Cheson BD, Nowakowski G, Salles G. Diffuse large B-cell lymphoma: new targets and novel therapies. Blood Cancer J. 2021;11(4):68.
5. Polson AG, Yu SF, Elkins K, Zheng B, Clark S, Ingle GS, et al. Antibody-drug conjugates targeted to CD79 for the treatment of non-Hodgkin lymphoma. Blood. 2007;110(2):616–23.
6. Schuster SJ, Bishop MR, Tam CS, Waller EK, Borchmann P, McGuirk JP, et al. Tisagenlecleucel in adult relapsed or refractory diffuse large B-cell lymphoma. N Engl J Med. 2019;380(1):45–56.
7. Sehn LH, Herrera AF, Flowers CR, Kamdar MK, McMillan A, Hertzberg M, et al. Polatuzumab vedotin in relapsed or refractory diffuse large B-cell lymphoma. J Clin Oncol. 2020;38(2):155–65.
8. Elstrom RL, Martin P, Ostrow K, Barrientos J, Chadburn A, Furman R, et al. Response to second-line therapy defines the potential for cure in patients with recurrent diffuse large B-cell lymphoma: implications for the development of novel therapeutic strategies. Clin Lymphoma Myeloma Leuk. 2010;10(3):192–6.
9. Issa JP, Kantarjian HM. Targeting DNA methylation. Clin Cancer Res. 2009;15(12):3938–46.
10. Jones PA, Ohtani H, Chakravarthy A, De Carvalho DD. Epigenetic therapy in immune-oncology. Nat Rev Cancer. 2019;19(3):151–61.
11. Clozel T, Yang S, Elstrom RL, Tam W, Martin P, Kormaksson M, et al. Mechanism-based epigenetic chemosensitization therapy of diffuse large B-cell lymphoma. Cancer Discov. 2013;3(9):1002–19.
12. Treppendahl MB, Kristensen LS, Gronbaek K. Predicting response to epigenetic therapy. J Clin Invest. 2014;124(1):47–55.
13. Chiappinelli KB, Strissel PL, Desrichard A, Li H, Henke C, Akman B, et al. Inhibiting DNA methylation causes an interferon response in cancer via dsRNA including endogenous retroviruses. Cell. 2015;162(5):974–86.
14. Roulois D, Loo Yau H, Singhania R, Wang Y, Danesh A, Shen SY, et al. DNA-demethylating agents target colorectal cancer cells by inducing viral mimicry by endogenous transcripts. Cell. 2015;162(5):961–73.
15. Balch C, Nephew KP. Epigenetic targeting therapies to overcome chemotherapy resistance. Adv Exp Med Biol. 2013;754:285–311.
16. Ronnekleiv-Kelly SM, Sharma A, Ahuja N. Epigenetic therapy and chemosensitization in solid malignancy. Cancer Treat Rev. 2017;55:200–8.
17. Qin T, Si J, Raynal NJ, Wang X, Gharibyan V, Ahmed S, et al. Epigenetic synergy between decitabine and platinum derivatives. Clin Epigenetics. 2015;7:97.
18. Matei D, Fang F, Shen C, Schilder J, Arnold A, Zeng Y, et al. Epigenetic resensitization to platinum in ovarian cancer. Cancer Res. 2012;72(9):2197–205.
19. Steinhardt JJ, Gartenhaus RB. Epigenetic approaches for chemosensitization of refractory diffuse large B-cell lymphomas. Cancer Discov. 2013;3(9):968–70.
20. Tsai HC, Li H, Van Neste L, Cai Y, Robert C, Rassool FV, et al. Transient low doses of DNA-demethylating agents exert durable antitumor effects on hematological and epithelial tumor cells. Cancer Cell. 2012;21(3):430–46.
21. Crump M, Baetz T, Couban S, Belch A, Marcellus D, Howson-Jan K, et al. Gemcitabine, dexamethasone, and cisplatin in patients with recurrent or

Liu *et al. Clinical Epigenetics*   (2023) 15:75

Page 18 of 18

refractory aggressive histology B-cell non-Hodgkin lymphoma: a phase II study by the National Cancer Institute of Canada Clinical Trials Group (NCIC-CTG). Cancer. 2004;101(8):1835–42.

22. Liston DR, Davis M. Clinically relevant concentrations of anticancer drugs: a guide for nonclinical studies. Clin Cancer Res. 2017;23(14):3489–98.

23. Leung KK, Nguyen A, Shi T, Tang L, Ni X, Escoubet L, et al. Multiomics of azacitidine-treated AML cells reveals variable and convergent targets that remodel the cell-surface proteome. Proc Natl Acad Sci U S A. 2019;116(2):695–700.

24. Rycaj K, Plummer JB, Yin B, Li M, Garza J, Radvanyi L, et al. Cytotoxicity of human endogenous retrovirus K-specific T cells toward autologous ovarian cancer cells. Clin Cancer Res. 2015;21(2):471–83.

25. Ku Y, Park JH, Cho R, Lee Y, Park HM, Kim M, et al. Noncanonical immune response to the inhibition of DNA methylation by Staufen1 via stabilization of endogenous retrovirus RNAs. Proc Natl Acad Sci U S A. 2021. https://doi.org/10.1073/pnas.2016289118.

26. Strissel PL, Ruebner M, Thiel F, Wachter D, Ekici AB, Wolf F, et al. Reactivation of codogenic endogenous retroviral (ERV) envelope genes in human endometrial carcinoma and prestages: emergence of new molecular targets. Oncotarget. 2012;3(10):1204–19.

27. Tokuyama M, Kong Y, Song E, Jayewickreme T, Kang I, Iwasaki A. ERVmap analysis reveals genome-wide transcription of human endogenous retroviruses. Proc Natl Acad Sci U S A. 2018;115(50):12565–72.

28. Schlee M, Hartmann G. Discriminating self from non-self in nucleic acid sensing. Nat Rev Immunol. 2016;16(9):566–80.

29. Liddicoat BJ, Piskol R, Chalk AM, Ramaswami G, Higuchi M, Hartner JC, et al. RNA editing by ADAR1 prevents MDA5 sensing of endogenous dsRNA as nonself. Science. 2015;349(6252):1115–20.

30. Schorn AJ, Gutbrod MJ, LeBlanc C, Martienssen R. LTR-retrotransposon Control by tRNA-derived small RNAs. Cell. 2017;170(1):61-71.e11.

31. Mi S, Lee X, Li X, Veldman GM, Finnerty H, Racie L, et al. Syncytin is a captive retroviral envelope protein involved in human placental morphogenesis. Nature. 2000;403(6771):785–9.

32. Villesen P, Aagaard L, Wiuf C, Pedersen FS. Identification of endogenous retroviral reading frames in the human genome. Retrovirology. 2004;1:32.

33. Mankan AK, Schmidt T, Chauhan D, Goldeck M, Honing K, Gaidt M, et al. Cytosolic RNA:DNA hybrids activate the cGAS-STING axis. EMBO J. 2014;33(24):2937–46.

34. Cheng Z, Dai T, He X, Zhang Z, Xie F, Wang S, et al. The interactions between cGAS-STING pathway and pathogens. Signal Transduct Target Ther. 2020;5(1):91.

35. Rigby RE, Webb LM, Mackenzie KJ, Li Y, Leitch A, Reijns MA, et al. RNA:DNA hybrids are a novel molecular pattern sensed by TLR9. EMBO J. 2014;33(6):542–58.

36. Krieg AM. Toll-like receptor 9 (TLR9) agonists in the treatment of cancer. Oncogene. 2008;27(2):161–7.

37. Fitzgerald KA, McWhirter SM, Faia KL, Rowe DC, Latz E, Golenbock DT, et al. IKKepsilon and TBK1 are essential components of the IRF3 signaling pathway. Nat Immunol. 2003;4(5):491–6.

38. Adams WJ, Aristoff PA, Jensen RK, Morozowich W, Romero DL, Schinzer WC, et al. Discovery and development of the BHAP nonnucleoside reverse transcriptase inhibitor delavirdine mesylate. Pharm Biotechnol. 1998;11:285–312.

39. Liu M, Ohtani H, Zhou W, Orskov AD, Charlet J, Zhang YW, et al. Vitamin C increases viral mimicry induced by 5-aza-2'-deoxycytidine. Proc Natl Acad Sci U S A. 2016;113(37):10238–44.

40. Liu J, Hong J, Han H, Park J, Kim D, Park H, et al. Decreased vitamin C uptake mediated by SLC2A3 promotes leukaemia progression and impedes TET2 restoration. Br J Cancer. 2020;122(10):1445–52.

41. Pera B, Tang T, Marullo R, Yang SN, Ahn H, Patel J, et al. Combinatorial epigenetic therapy in diffuse large B cell lymphoma pre-clinical models and patients. Clin Epigenetics. 2016;8:79.

42. Laurent A, Madigou T, Bizot M, Turpin M, Palierne G, Mahe E, et al. TET2-mediated epigenetic reprogramming of breast cancer cells impairs lysosome biogenesis. Life Sci Alliance. 2022. https://doi.org/10.26508/lsa.202101283.

43. Ma F, Li B, Yu Y, Iyer SS, Sun M, Cheng G. Positive feedback regulation of type I interferon by the interferon-stimulated gene STING. EMBO Rep. 2015;16(2):202–12.

44. Dai W, Xu Y, Mo S, Li Q, Yu J, Wang R, et al. GLUT3 induced by AMPK/CREB1 axis is key for withstanding energy stress and augments the efficacy of current colorectal cancer therapies. Signal Transduct Target Ther. 2020;5(1):177.

45. Tsogbadrakh B, Ryu H, Ju KD, Lee J, Yun S, Yu KS, et al. AICAR, an AMPK activator, protects against cisplatin-induced acute kidney injury through the JAK/STAT/SOCS pathway. Biochem Biophys Res Commun. 2019;509(3):680–6.

46. Levitt DG. PKQuest_Java: free, interactive physiologically based pharmacokinetic software package and tutorial. BMC Res Notes. 2009;2:158.

47. Gong C, Qian L, Yang H, Ji LL, Wei H, Zhou WB, et al. Hepatotoxicity and pharmacokinetics of cisplatin in combination therapy with a traditional Chinese medicine compound of Zengmian Yiliu granules in ICR mice and SKOV-3-bearing nude mice. BMC Complement Altern Med. 2015;15:283.

48. Liu J, Hong J, Ahn KS, Go J, Han H, Park J, et al. ERK-dependent IL-6 positive feedback loop mediates resistance against a combined treatment using danusertib and BKM120 in Burkitt lymphoma cell lines. Leuk Lymphoma. 2019;60(10):2532–40.

49. Gentleman RC, Carey VJ, Bates DM, Bolstad B, Dettling M, Dudoit S, et al. Bioconductor: open software development for computational biology and bioinformatics. Genome Biol. 2004;5(10):R80.

Publisher's Note